© JUN 2026 | IRE Journals | Volume 9 Issue 12 | ISSN: 2456-8880
DOI: https://doi.org/10.64388/IREV9I12-1718964

Comparative Assessment of Background Ionizing Radiation Levels and Public Safety Limits in Modern and Traditional Buildings of Kurudu, Abuja

JOSEPH TERYIMA IORTILE
Department of Physics, Faculty of Sciences, National Open University of Nigeria, Abuja

Abstract- This study evaluated and compared background ionizing radiation (BIR) levels within modern and traditional buildings in Kurudu. The assessment targeted twenty locations per building category, computing the Indoor Annual Effective Dose Rate (IAEDR) and Outdoor Annual Effective Dose Rate (OAEDR) to establish the total effective dose rate. For modern structures, the background radiation dose rate ranges yielded an overall mean IAEDR of 1.32 ± 0.01 mSv/yr, and OAEDR of 0.27 ± 0.01 mSv/yr, and a total effective dose rate of 1.59 ± 0.01 mSv/yr. Conversely, traditional structures exhibited lower background values, maintaining an overall mean IAEDR of 1.02 ± 0.01 mSv/yr, and OAEDR of 0.34 ± 0.01 mSv/yr, and a total effective dose rate of 1.37 ± 0.02 mSv/yr. While the majority of isolated readings remain safely bounded, the accumulated total effective dose rates in both building types exceeded the standard public safety limit of 1.0 mSv/yr established by the International Commission on Radiological Protection (ICRP). However, the values fall well within the broader global background radiation safety ceiling of 2.4 to 3.0 mSv/yr outlined by the United Nations Scientific Committee on the Effects of Atomic Radiation (UNSCEAR).

Keywords: Background Ionizing Radiation, Annual Effective Dose Rate (AEDR), Modern and Traditional Buildings, Public Safety Limits, Kurudu

I. INTRODUCTION

Background radiation refers to the ionizing radiation that persistently exists in the environment and to which all people are continuously exposed without deliberate introduction of radioactive sources. It comprises radiation from both natural and artificial sources, although natural sources account for the largest proportion of exposure worldwide (EPA, 2025). The sources of background radiation include cosmic radiation (primary and secondary), terrestrial radiation (from natural radium, uranium, and thorium and their decay products; radon gas which is the largest natural source of radiation exposure to human beings), internal radiation (radioactivity in the body) (Yahaya et al., 2024).

Artificial or man-made sources occur mainly from medical exposure, weapon testing, nuclear technologies and use of office equipment (Chiegwu, et al., 2022). Approximately 85% of the annual total radiation dose of any person comes from natural radionuclides of both terrestrial and cosmogenic origin (USNRC, 2023).

The worldwide average annual effective dose from natural background radiation is approximately 2.4 millisierverts (mSv) per year, but this value varies widely depending on geologic and geographic conditions. Typical ranges are between 1 to 10mSv per year, with significantly higher levels recorded in certain regions due to elevated radon concentrations or remarkably radioactive geology (World Nuclear Association, 2025).

Outdoor external radiation is driven by trace levels of terrestrial radionuclides found across all soil profiles. Gamma rays produced within the top 15–30 cm of soil can penetrate upward to reach the Earth's surface. Only primordial radionuclides with half-lives matching the planet's age, along with their associated decay chains, persist in quantities large enough to contribute significantly to this environment (Petrović et al., 2025).

Quantifying this ionizing radiation exposure remains a fundamental objective for radiation protection experts and regulatory authorities. For public health frameworks managing radiation emergencies, baseline environmental data is critical to rapidly assess, model, and categorize exposure (Weerakkody et al, 2022).

Furthermore, atmospheric dynamics can transport these radioactive particles and gases across vast geographic distances. Indoors, the ambient gamma absorbed dose rate typically spans 20 to 190 nGy/h, exhibiting a global population-weighted baseline average of approximately 80 to 84 nGy/h (Kim et al, 2025). A key byproduct of these heavy natural decay chains is radon gas. Inhalation of indoor radon is a premier environmental health hazard; it constitutes the primary cause of lung cancer among non-smokers and stands as the second leading cause of lung cancer globally, surpassed only by tobacco use (Chen et al., 2023).

This study is therefore intended to evaluate the indoor and outdoor background ionizing radiation across modern and traditional residences within Kurudu, Abuja, establishing a critical radiological baseline by calculating the absorbed dose rates and Annual Effective Dose Equivalent (AEDE), the findings will safeguard local construction practices align with UNSCEAR and ICRP safety standards.

II. MATERIALS AND METHODS

Material

The Radiation Alert Inspector EXP+ (Serial Number 24650) is a highly sensitive, USA-manufactured digital handheld radiation survey meter designed by SE International to detect low levels of ionizing alpha, beta, gamma, and X-ray radiation. The external probe uses an external detachable wand on a flexible cable to check tight spaces and surfaces. Weighing approximately 273 grams for the main body and 328 grams for the external probe assembly, this rugged meter offers an exceptional gamma sensitivity of 3,340 to 3,500 counts per minute per milliroentgen per hour (CPM/mR/hr) referenced to Cesium-137.

It is powered by a standard single 9-volt alkaline battery, which delivers an impressive capacity of roughly 2,160 hours of continuous operation under normal background conditions. It's broad operating range measures exposure from 0.001 to 100 mR/hr (or 0.01 to 1,000 μSv/hr) and pulse counts from 0 to 350,000 CPM (or 0 to 5,000 CPS).

Figure 1: Alert Meter, Inspector EXP+

III. METHOD

To measure radiation levels, an Inspector EXP+ alert meter was powered on through the switch button, and its external probe was opened. The meter was held vertically upward at a height of 1 meter above the ground to align the device window with incoming radiation and capture the average exposure level of the human body. The assessment covered forty (40) locations in total: twenty indoor and twenty outdoor environments, spanning both traditional and modern building designs.

To ensure a representative sample, five distinct readings were recorded in micro-Sieverts per hour (μSv/hr) at each location. Indoor measurements were taken with the meter directly facing the building walls to ensure accuracy for average calculations. Conversely, outdoor background readings were collected as far away from the building walls as possible. The equations below were used to analyze the results.

$$IAEDR\,\frac{mSv}{yr} = (EDR) \times 8760\,\frac{hr}{yr} \times 0.8 \div 1000 \quad (1)$$

$$OAEDR\frac{mSv}{yr} = (EDR) \times 8760\frac{hr}{yr} \times 0.2 \div 1000 \quad (2)$$

$$TAEDR\frac{mSv}{yr} = OAEDR + IAEDR \quad (3)$$

IV. RESULTS AND DISCUSSION

Table 1: Summary of background Radiation Levels for Selected location in Kurudu Modern buildings

Area code	Mean X($\mu Sv/hr$)	Mean Y($\mu Sv/hr$)	IAEDR mSv/yr	OAEDR mSv/yr	Total effective dose rate mSv/yr
K1	0.161±0.01	0.141± 0.01	1.13±0.01	0.25± 0.01	1.38± 0.01
K2	0.180±0.02	0.151±0.01	1.26±0.02	0.26± 0.01	1.52± 0.01
K3	0.192±0.01	0.162±0.01	1.35±0.01	0.28± 0.01	1.63± 0.01
K4	0.221±0.03	0.170±0.01	1.55±0.03	0.29± 0.01	1.84± 0.01
K5	0.160±0.01	0.160±0.01	1.12±0.01	0.28± 0.01	1.40± 0.01
K6	0.182±0.02	0.150±0.01	1.28±0.02	0.26± 0.01	1.54± 0.01
K7	0.192±0.01	0. 141±0.01	1.35±0.01	0.25± 0.01	1.60± 0.01
K8	0.222±0.02	0.170±0.02	1.56±0.02	0.29± 0.02	1.85± 0.02
K9	0.161±0.01	0.160±0.01	1.13±0.01	0.28± 0.01	1.41± 0.01
K10	0. 182±0.02	0.161±0.01	1.28±0.02	0.28± 0.01	1.56± 0.01
K11	0.193±0.02	0.130±0.01	1.35±0.02	0.23± 0.01	1.58± 0.01
K12	0.221±0.02	0.140±0.01	1.55±0.02	0.25± 0.01	1.80± 0.01
K13	0.160±0.01	0. 150±0.01	1.12±0.01	0.26± 0.01	1.38± 0.01
K14	0. 181±0.02	0.160±0.01	1.27±0.02	0.28± 0.01	1.55± 0.01
K15	0.191±0.02	0.170±0.02	1.34±0.02	0.29± 0.02	1.63± 0.02
K16	0.221±0.03	0.160±0.01	1.55±0.03	0.28± 0.01	1.83± 0.01
K17	0.161±0.01	0.150±0.01	1.13±0.01	0.26± 0.01	1.39± 0.01
K18	0. 180±0.02	0. 141±0.01	1.26±0.02	0.25± 0.01	1.51± 0.01
K19	0.191±0.01	0.170±0.02	1.34±0.01	0.29± 0.02	1.63± 0.02
K20	0.220±0.02	0.161±0.01	1.54±0.02	0.28± 0.01	1.82± 0.01
Mean			1.32± 0.01	0.27± 0.01	1.59± 0.01

Table 2: Summary of background Radiation Levels
for Selected location in Kurudu Traditional buildings

Area code	Mean X($\mu Sv/hr$)	Mean Y($\mu Sv/hr$)	IAEDR mSv/yr	OAEDR mSv/yr	Total effective dose rate mSv/yr
KH1	0.140±0.01	0.141± 0.01	0.98±0.01	0.25±0.01	1.23±0.01
KH2	0.150±0.02	0.130±0.01	1.05±0.02	0.23±0.01	1.28±0.02
KH3	0.140±0.01	0.130±0.01	0.98±0.01	0.23±0.01	1.21±0.01
KH4	0.130±0.03	0.130±0.01	0.91±0.03	0.23±0.01	1.14±0.02
KH5	0.150±0.01	0.160±0.01	1.05±0.01	0.28±0.01	1.33±0.01
KH6	0.150±0.02	0.130±0.01	1.05±0.02	0.23±0.01	1.28±0.02
KH7	0.160±0.01	0. 140±0.01	1.12±0.01	0.25±0.01	1.37±0.01
KH8	0.150±0.02	0.130±0.02	1.05±0.02	0.23±0.02	1.28±0.02
KH9	0.131±0.01	0.140±0.01	0.92±0.01	0.25±0.01	1.17±0.01
KH10	0. 150±0.02	0.130±0.01	1.05±0.02	0.23±0.01	1.28±0.02
KH11	0.140±0.02	0.120±0.01	0.98±0.02	0.84±0.01	1.82±0.02
KH12	0.150±0.02	0.140±0.01	1.05±0.02	0.25±0.01	1.30±0.02
KH13	0.160±0.01	0. 150±0.01	1.12±0.01	0.26±0.01	1.38±0.01
KH14	0. 151±0.02	0.140±0.01	1.06±0.02	0.25±0.01	1.31±0.02
KH15	0.151±0.02	0.130±0.02	1.06±0.02	0.23±0.02	1.29±0.02
KH16	0.140±0.03	0.131±0.01	0.98±0.03	0.92±0.01	1.90±0.02
KH17	0.151±0.01	0.130±0.01	1.06±0.01	0.23±0.01	1.29±0.01
KH18	0. 140±0.02	0. 141±0.01	0.98±0.02	0.99±0.01	1.97±0.02
KH19	0.150±0.01	0.132±0.02	1.05±0.01	0.23±0.02	1.28±0.02
KH20	0.141±0.02	0.132±0.01	0.99±0.02	0.23±0.01	1.22±0.02
Mean			1. 02 ±0.01	0.34±0.01	1.37±0.02

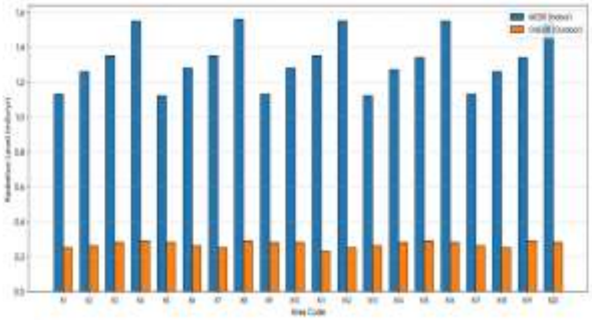

Figure 1: Comparison of indoor (IAEDR) and Outdoor (OAEDR) Annual Effective Dose Rates for modern buildings

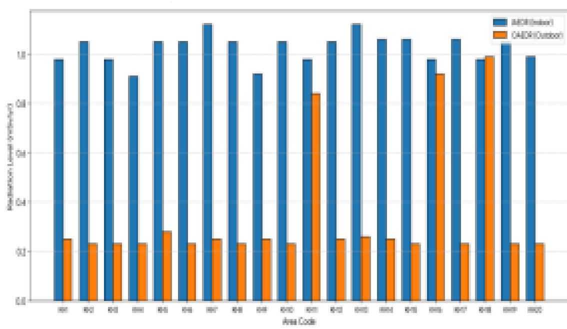

Figure 2: Comparison of indoor (IAEDR) and Outdoor (OAEDR) Annual Effective Dose Rates for traditional buildings

The assessment of background ionizing radiation (BIR) inside residential spaces is critical for enumerating the health risks associated with chronic public exposure to natural terrestrial radionuclides. The empirical findings in Tables 1 and 2 highlight significant structural discrepancies in radiation profiles between modern and traditional buildings across Kurudu.

Table 1 shows the modern residential dwellings K1 to K20 demonstrated a heightened radiation profile. The Indoor Annual Effective Dose Rate (IAEDR) varied between a minimum of 1.12 ± 0.01 mSv/yr at K5 and K13 and a maximum of 1.56 ± 0.02 mSv/yr at K8. The Outdoor Annual Effective Dose Rate (OAEDR) ranged from 0.23 ± 0.01 mSv/yr at K11 to 0.29 ± 0.02 mSv/yr at K4, K8, and K15 as shown in Figure 1. Summing these pathways yielded an overall total effective dose rate mean of 1.59 ± 0.01 mSv/yr.

This elevated indoor baseline is tied directly to modern masonry components. Materials such as cement blocks, concrete aggregate, decorative ceramic tiles, and granite stones carry elevated concentrations of primordial radionuclides 226Ra, 232Th, and 40K. When these components are densely incorporated into modern building shells, they accelerate internal gamma emission rates and trap radon progeny, inflating indoor readings well past outdoor levels (Synnott et al., 2025).

Traditional architectural structures KH1 to KH20 showed a fundamentally different radiological distribution (Table 2). The IAEDR values spanned from 0.91 ± 0.03 mSv/yr at KH4 up to 1.12 ± 0.01 mSv/yr at KH7 and KH13, culminating in a mean IAEDR of 1.02 ± 0.01 mSv/yr. Interestingly, the mean OAEDR was found to be 0.34 ± 0.01 mSv/yr, with specific spikes hitting 0.84 ± 0.01 mSv/yr at KH11, 0.92 ± 0.01 mSv/yr at KH16, and 0.99 ± 0.01 mSv/yr at KH18 as shown across the radiation levels in Figure 2.

The reduced indoor radiation levels in traditional buildings stem from the organic nature of their primary construction materials, which consist of mud, thatch, and wood. These earth-based compounds inherently showcase lower gamma emission rates compared to heavily processed industrial concrete.

However, the outdoor spikes seen at spots like KH11, KH16, and KH18 suggest that the surrounding surface soil in those specific clusters contains naturally richer deposits of monazite or radioactive rock outcrops (Jammaz, 2024). The ICRP recommends an annual public exposure limit of 1.0 mSv/yr. The total effective dose rates in modern zones 1.59mSv/yr and traditional zones 1.37 mSv/yr both exceeds this threshold. Because the calculated totals from Kurudu do not eclipse the upper limits of the global background scale 3.0 mSv/yr, residents face no immediate or severe radiological health crises.

CONCLUSION

The assessment of background ionizing radiation in Kurudu indicates that modern dwellings present higher indoor dose rates, averaging up to 1.59 mSv/yr, due to the presence of primordial radionuclides in masonry materials like concrete, granite, and tiles. Conversely, traditional mud and thatch structures maintain lower indoor radiation levels but exhibit higher outdoor anomalies, highlighting that architectural design and material selection are key drivers of public exposure to natural radioactivity.

Both modern and traditional housing zones exhibit combined total effective dose rates exceeding the 1.0 mSv/yr annual limit recommended by the International Commission on Radiological Protection (ICRP). While this suggests the need for improved ventilation in modern structures, the levels remain below the 3.0 mSv/yr upper threshold of global background radiation, meaning residents face no immediate radiological health crises, though ongoing monitoring is recommended.

REFERENCES

[1] Chen, X., Wang, Y., & Zhang, L. (2023). Risk assessment of lung cancer caused by indoor radon exposure in contemporary residential architecture. International Journal of Environmental Public Health, 2023, Article 6943333.

[2] Chiegwu, H. U., Onyeka, J. O., Ugwuanyi, D. C., Odunk, D. D., Ogolodom, M. P., & Mbaba, A. N. (2022). Assessment of background ionizing radiation exposure levels in industrial buildings in Nnewi, Anambra State, Nigeria. International Journal of Research in Medical Sciences, 10(2), 305–315

[3] Environmental Protection Agency. (2025). Radiation sources and doses. U.S. Environmental Protection Agency. https://www.epa.gov/radiation/radiation-sources-and-doses

[4] Jammaz, A. M. (2024). Evaluation of the radiation emission of radon gas from various building materials using solid-state nuclear track detectors. Journal of King Saud University - Science, 36(6), 103214.

[5] Kim, S. H., Park, J. H., & Lee, K. W. (2025). Assessment of population exposure to terrestrial gamma radiation: National high-resolution mapping vs. global baselines. Radiation Protection Dosimetry, 199(14), 1542–1551.

[6] Petrović, J., Milanović, S., & Ćujić, M. (2025). Assessment of terrestrial radionuclide exposure and topsoil accumulation dynamics in diverse geomorphological zones. Journal of Environmental Radioactivity, 268, Article 107119.

[7] Synnott, H., Fenton, D., & Organo, C. (2025). Integrating Radon/Thoron and Gamma Radiation Exposure for a Comprehensive Dose Estimation Model for Building Materials. Applied Sciences, 15(12), 6470

[8] United States Nuclear Regulatory Commission. (2023). Ionizing radiation. https://www.nrc.gov/reading-rm/basicref/glossary/ionizing-radiation.html

[9] Weerakkody, T., Williams, S., & Warnakulasuriya, T. (2022). Assessment of background radiation and associated dose rates for environmental emergency risk zoning. Journal of Geoscience and Environment Protection, 10(10), 12–25.

[10] World Nuclear Association. (2025). World Nuclear Outlook Report 2025. world-nuclear.org

[11] Yahaya, M. N., Emmanuel, C. C., Samaila, B., Bako, A., & Isa, H. (2024). Assessment of indoor and outdoor ambient radiation levels at Federal University Birnin Kebbi, Kebbi State. Savanna Journal of Basic and Applied Sciences, 6(2), 230–237.